



Semnan University

Mechanics of Advanced Composite Structures

journal homepage: <http://MACS.journals.semnan.ac.ir>

Material Mechanical Properties Prediction of Layer with Multidirectional Fiber Ply Reinforced Polymer Matrix Composites

M.M. Hassan^{a*}, A.B. Siddique^b, B. Bohanon^c

^a Department of Nanoscience and Microsystem Engineering, University of New Mexico, Albuquerque, NM, USA

^b Department of Mechanical Engineering, University of New Mexico, Albuquerque, NM, USA

^c Department of Nuclear Engineering, University of New Mexico, Albuquerque, NM, USA

KEYWORDS

Reinforced polymer;
Multidirectional fiber;
Mechanical properties;
Tsai-Wu failure criteria;
Finite element analysis.

ABSTRACT

Carbon fiber reinforced plastics (CFRP) are now being used in primary structures of airplanes, ships, and automotive engineering and for applications that demand sustained high reliability and strength during long-term operations. The present work provides a three-dimensional (3D) model that has been established for the simulation of the multidirectional carbon fiber reinforced plastic (CFRP) composite layer which enables understanding of the mechanical properties at failure using finite element simulation software ANSYS. The matrix is considered isotropic and elastic-plastic. Moreover, the carbon fiber is considered transversely isotropic and linear elastic for the finite element modeling. The maximum stress-strain criterion is used to determine the failure of fiber and matrix of composite layer for both analytical and modeling analysis. The modeling result shows that the elastic modulus in fiber orientation is significantly higher. Numerical and analytical results of nonlinear mechanical stress and the distribution on the multilayer show good agreement with experimental results.

1. Introduction

Fiber-reinforced polymer composites (FRP) are the most vastly used composite materials actually and research on FRP composites has been increasingly developed due to their ample structural potential [1]. FRP composites have steadily gained various applications in different fields. The modern concept and technology of fiber-reinforced polymer composites have accompanied ample change with the clear concept of composite laminates [2]. As advanced engineering materials, Composite laminates have many applications primarily as components in aircraft, ships, cars, rail vehicles, power plants, civil engineering structures, robots, prosthetic devices, sports equipment, etc. [3-5]. The reasons behind this huge demand are mainly due to the high strength-to-weight ratio, adjustable mechanical properties, and fatigue resistance [6].

The elastic properties of composite layers depend on multifarious factors like the configuration of the laminates, materials used,

and the production method. Laminated material with the required strength and stiffness characteristics with respect to specific design conditions can be determined by a different arrangement of layers and fiber directions [7]. The mechanical and elastic properties of composites are not fixed until the final structure is manufactured. These characteristics could be achieved by employing standardized tests or with numerical methods [8-10]. Due to the expenses and inconveniences in experimental methods, it is more common to estimate these properties by numerical calculations.

The elastic properties of composites are determined by the mechanical characteristics of the constituent materials. In order to predict and characterize composite behavior, different analytical and numerical techniques have been applied [11][12][13]. Analytical solutions do not always provide good results due to the complexity and the number of equations arising from complex geometries, loading conditions, and material characteristics [14-16]. Extracting

* Corresponding author. Tel.: +1-505-277-6824
E-mail address: mdmehadihassan@unm.edu

effective elastic properties is the main requirement in studying the mechanics of composite materials.

The tensile properties of fiber-reinforced composites polymer are affected by several factors, such as fiber-matrix interaction, volume fraction, aspect ratio (diameter to length of fiber), fiber orientation, and rules of the mixture model [17-19]. Rehan et al. [20] investigated the fiber orientation effects of multidirectional composite laminates with special stacking sequences leading to isolating the orientation parameter at the crack interface. The stacking structures also influenced on mechanical properties of carbon fiber/epoxy IM7/937-7 laminates and carbon/glass interlayer hybrid composite was investigated by Roy et al. [21] and Weili et al. [22] respectively. They found that the mechanical properties as tensile and compressive moduli increase for hybrid composite with the increase of fiber concentration. Daniel et al. [23] proposed a failure theory to predict the lamina strength under multi-axial stress on the strain rate effect. The axial and radial stress was calculated as a function of axial distance in an elastic fiber surrounded by a plastic matrix by the finite element method and the results demonstrated that the axial stress increased linearly from the end towards the center; the radial stress was more evenly distributed [24]. Xi Deng et al. [25] proposed a new three-dimensional micromechanical model for the analysis of multidirectional fiber of reinforced polymer and showed a good agreement with the experimental results. The local fiber deformations and micro-debonding between matrix and fibers are caused by void influence on composite tensile strength investigated by Olivier et al. [26]. Another researcher Nirbhay et al.[27] investigated the strength of composite with various stacking sequences of carbon fiber and found that the carbon fiber with cross-ply lamination is stiffer than the angle ply glass fiber lamination.

If the fibers are parallel with the direction of loading, the optimum stiffness and strength can be achieved, On the other hand, when the fibers are perpendicular to the direction of applied load, then the strength of the composite is comparatively low. However, fibers can vary in different orientations as 90°, 45°, or 30° angles to accommodate for the direction of the applied loads to give better strength. This article aims to predict the material property of a layer with multi-directional fiber ply reinforced polymer matrix composites. A composite layer consists of multiple numbers of ply that have been used to perform different tests (tensile, expansion, or shear) using the finite element analysis software ANSYS. Some predefined material properties were taken and simulation was carried out with

the specific number of plies and their regular alternating orientation. The deviation between numerical results and modeling results of elastic modulus and share modulus were calculated.

2. Governing Equations in Finite Element Analysis

Fibers are randomly oriented in composite material. Material properties are varied for different arrangements of the fibers. The stress-strain equation for a transversely isotropic material in the elastic region follows Hook's law and the relationship can be written as [28].

$$\begin{Bmatrix} \varepsilon_x \\ \varepsilon_y \\ \varepsilon_z \\ \gamma_{xy} \\ \gamma_{yz} \\ \gamma_{zx} \end{Bmatrix} = \begin{bmatrix} \frac{1}{E_x} & -\frac{\nu_{xy}}{E_y} & -\frac{\nu_{xz}}{E_z} & 0 & 0 & 0 \\ -\frac{\nu_{yx}}{E_x} & \frac{1}{E_y} & -\frac{\nu_{yz}}{E_z} & 0 & 0 & 0 \\ -\frac{\nu_{zx}}{E_x} & -\frac{\nu_{zy}}{E_y} & \frac{1}{E_z} & 0 & 0 & 0 \\ 0 & 0 & 0 & \frac{1}{G_{xy}} & 0 & 0 \\ 0 & 0 & 0 & 0 & \frac{1}{G_{yz}} & 0 \\ 0 & 0 & 0 & 0 & 0 & \frac{1}{G_{zx}} \end{bmatrix} \begin{Bmatrix} \sigma_x \\ \sigma_y \\ \sigma_z \\ \tau_{xy} \\ \tau_{yz} \\ \tau_{zx} \end{Bmatrix} \quad (1)$$

where, $\varepsilon_x, \varepsilon_y$ and ε_z are the stress in x, y, and z-direction. γ_{xy}, γ_{yz} and γ_{zx} are the strain in x, y, and z-direction. The z-axis is considered the fiber direction and the x-y plane is the transverse basal plane. The share modulus of x, y and z directions is G_{xy}, G_{yz} and G_{zx} . If the normal stress σ_x acts in the x-direction, the elastic modulus E_x is defined as

$$E_x = \frac{\sigma_x}{\varepsilon_x} = \left(\frac{L}{\Delta L}\right) \sigma_x \quad (2)$$

$$\nu_{xy} = \nu_{yx}, \nu_{zx} = \nu_{zy}, \nu_{xz} = \nu_{yz}$$

Composite laminate has individual layers consisting of unilateral plies with the same or regularly alternating orientation as shown in Fig. 1. The layers can also be applied from thermosetting or thermoplastic polymers, metals, and fabric or have a spatial 3-D reinforced structure.

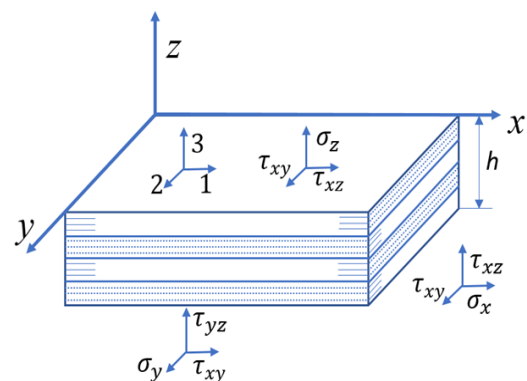


Fig. 1. Graphical representation of the composite layer

If the layer consists of m longitudinal plies oriented at 0° with the thickness $h_0(i)$ ($i=1,2,3,\dots,m$) and n transverse plies with 90° with the thickness $h_{90}(j)$ ($j=1,2,3,\dots,n$) are made of the same composite materials. Next, stresses σ_x, σ_y and τ_{xy} form the plane stress state in the global coordinate frame and can be transformed in terms of stresses in the principal coordinates of the plies as the equation given below whereas the total thickness is $h = h_0 + h_{90}$, $h_0 = \sum_{i=1}^m h_0^i$, $h_{90} = \sum_{j=1}^n h_{90}^j$. The h_0 and h_{90} are the longitudinal and transverse thickness of ply respectively.

$$\begin{aligned} \sigma_x h &= \sum_{i=1}^m \sigma_1^i h_0^i + \sum_{j=1}^n \sigma_2^j h_{90}^j, \\ \sigma_y h &= \sum_{i=1}^m \sigma_2^i h_0^i + \sum_{j=1}^n \sigma_1^j h_{90}^j, \\ \tau_{xy} h &= \sum_{i=1}^m \tau_{12}^i h_0^i + \sum_{j=1}^n \tau_{12}^j h_{90}^j \end{aligned} \tag{3}$$

Similarly, the Stresses in the principal coordinates of the plies are related to the corresponding strains given below.

$$\begin{aligned} \sigma_1^{(i,j)} &= \bar{E}_1 (\varepsilon_1^{(i,j)} + \nu_{12} \varepsilon_2^{(i,j)}), \\ \sigma_2^{(i,j)} &= \bar{E}_2 (\varepsilon_2^{(i,j)} + \nu_{21} \varepsilon_1^{(i,j)}), \\ \tau_{12}^{(i,j)} &= G_{12} \gamma_{12}^{(i,j)} \end{aligned} \tag{4}$$

2.1. Maximum Stress Failure Theory

The stresses acting on a lamina in the local axis are of two types i.e., the normal and shear stress. So the lamina will fail if each of the local axes' normal or shear stresses is equal to or exceeds the corresponding ultimate strengths of the unidirectional lamina [29]. When these components are higher than the corresponding tension or compression yield strength, then the failure occurs. The σ_1^c and σ_1^t symbols represent the normal stress corresponding to compression and tension respectively.

$$\begin{aligned} -(\sigma_1^c)_{ult} &< \sigma_1 < (\sigma_1^t)_{ult}, \text{ or} \\ -(\sigma_2^c)_{ult} &< \sigma_2 < (\sigma_2^t)_{ult}, \text{ or} \\ -(\tau_{12})_{ult} &< \tau_{12} < (\tau_{12})_{ult} \end{aligned} \tag{5}$$

The most common failure criterion used to predict the failure of composite materials is the maximum stress criterion which is a linear, stress-based, and failure mode dependent criterion without stress interaction [30]. The failure index of a lamina is given by equation No. 4 using the maximum stress failure theory.

2.2. Maximum Strain Failure Theory

The lamina strains are resolved in the local axes. A lamina will fail if these normal or shear strains are equal to or exceed the corresponding ultimate strains of the unidirectional lamina. The ε_1^c and ε_1^t symbols represent the normal strain corresponding to compression and tension respectively.

$$\begin{aligned} -(\varepsilon_1^c)_{ult} &< \varepsilon_1 < (\varepsilon_1^t)_{ult}, \text{ or} \\ -(\varepsilon_2^c)_{ult} &< \varepsilon_2 < (\varepsilon_2^t)_{ult}, \text{ or} \\ -(\gamma_{12})_{ult} &< \gamma_{12} < (\gamma_{12})_{ult} \end{aligned} \tag{6}$$

The failure index of a lamina is given by equation no.7 using the maximum strain failure theory.

$$I_F = \max \begin{cases} \varepsilon_1 / \varepsilon_{1t} \text{ if } \varepsilon_{1t} > 0 \text{ or } -\varepsilon_1 / \varepsilon_{1c} \text{ if } \varepsilon_1 < 0 \\ \varepsilon_2 / \varepsilon_{2t} \text{ if } \varepsilon_{2t} > 0 \text{ or } -\varepsilon_2 / \varepsilon_{2c} \text{ if } \varepsilon_2 < 0 \\ \varepsilon_3 / \varepsilon_{3t} \text{ if } \varepsilon_{3t} > 0 \text{ or } -\varepsilon_3 / \varepsilon_{3c} \text{ if } \varepsilon_3 < 0 \\ \text{abs}(\gamma_4) / \gamma_{4U} \\ \text{abs}(\gamma_5) / \gamma_{5U} \\ \text{abs}(\gamma_6) / \gamma_{6U} \end{cases} \tag{7}$$

3. Finite Element Modeling

Finite element analysis is one of the most powerful tools for the design and analysis of any complex problem. It involves the approximation of a continuous function by a discrete model and the deformation of physical solids whereas, the whole body of the model is divided into several smaller parts considered as elements that are interconnected with the nodes. The steps for the finite element modeling are shown in Fig. 2. The commercial FEA ANSYS software (Canonsburg, Pennsylvania) was used for finite element modeling.

PLANE183, an Axi-symmetric 8-node element type was used as carbon fiber. The quadratic displacement behavior was exhibited by SOLID186, a homogeneous structural Solid is a higher-order three-dimensional 20-node solid element. The element was defined by 20 nodes with three degrees of freedom (x, y and z) per each one. The elements had nonlinear capabilities, such as large deflection, large strain, and elastic-plastic stress-strain of the material constitutive. The finite element model dimensions orders were several hundred times smaller than real specimens due to computation time limitations and finer element requirements for better accuracy. The length and width of each layer were 5mm and 5 mm. The thickness of the individual layer was 0.5 mm. The total number of

layers/ply was 20 due to the limitation of computing time of the ANSYS software version. The fibers were in the X direction in the odd layers and for the case of even layers, the fibers were in the Y direction. The angle between the two plies was 90°. In order to carry the various internal and external loads applied, fibers can be positioned in any direction within the tube. The proper element size and density were determined by convergence study of the tensile test so that the model in Fig. 3 is mesh-independent. The matrix's total number of elements is 6000 and the number of nodes is 28,060. The element meshing was very important to improve the accuracy of the FEM shown in Fig. 4. Applying the boundary conditions was the most crucial part of the simulation. Boundary conditions virtually and mathematically simulate the theoretical test conditions. It helped to understand the basics and actual working of the tests. All boundary conditions have been applied to the solid model for the tensile test by setting the X, Y and Z plane fixed on one side and making the strain on another side 1.

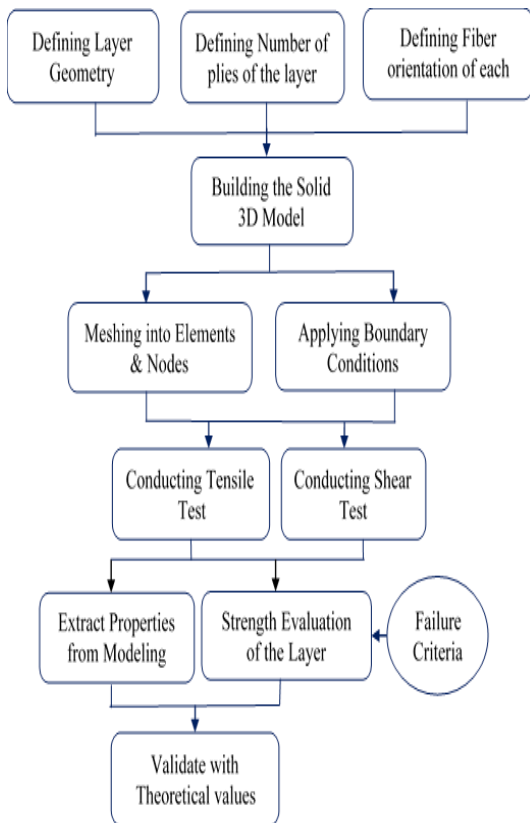


Fig. 2. Flow chart for finite element modeling

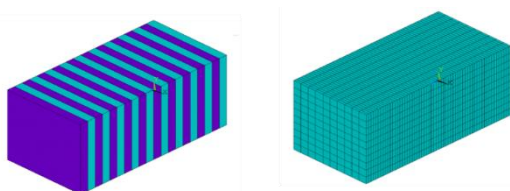


Fig. 3. (Left) FEA 3D model of 20 layers and (Right) Mesh of the model (Isometric View)

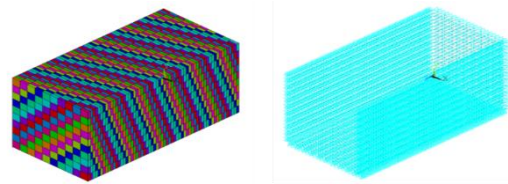


Fig. 4. (Left) Element meshing of the 3D model, and (Right) Boundary condition applied on the Meshing of the model (Isometric View)

4. Modeling Result and Discussion

The volume fraction of the fiber and matrix in composite material plays an important role in shaping its properties. The fiber attributes almost 80% to 90% of the properties of the composite material again it also depends on the volume fraction of the fiber too. A regular three-dimensional long fiber in a matrix was used to describe the volume fraction of the single layer of the composite as shown in Fig. 5. The mechanical properties of carbon fiber and epoxy are given in Table 1 [31]. The nominal diameter of the carbon fiber was 5–10 μm and it was composed mostly of carbon atoms. The total number of nodes and elements was 19,822 and 3,870 were used for a single fiber. From the volume fraction, the sides of the square i.e. length and width of the matrix were calculated using the following relation as $w = \sqrt{\pi/v_{frctn}} \cdot r$ where w is the width of a square matrix of the representative element, v_{frctn} is the volume fraction of fiber and r is the radius of the fiber. After the tensile test through the modeling, the stress and young's modulus in the axial direction of Z was calculated at 137 GPa with a strain of 0.01%. The maximum Von Mises stress is found at 2.5 GPa. The Von Mises stress is used to determine whether an isotropic and ductile metal will yield a complex loading condition or not. In addition, the Poisson's ratio of composite material for strain-induced in x and y direction because of the force in z-direction i. e. $\nu_{12} = \nu_x / \nu_z$ and $\nu_{13} = \nu_y / \nu_z$, where Z_1 is fiber direction and X_2 & Y_3 are transverse directions. Finally, the numerical calculation of the elastic modulus, $E_1 = E_f \cdot v_f + E_m \cdot v_m$; (f and m denote fiber and matrix) is 155.77GPa which validates the simulation results in the volume fraction of 0.62. The elastic properties of fiber content in single-ply are shown in Fig. 6 with different volume fractions.

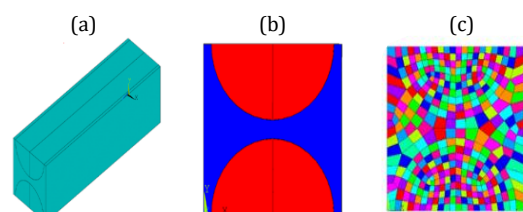


Fig. 5. Unit cell of square array fiber packing geometry in 3D (a) for one-fiber (b) Von Mises stress distribution and (c) FEA mesh both fiber and matrix (Front view)

Table 1. Geometrical characteristics of the specimens

Materials	Elastic Moduli		Poisson's Ratio			Share Moduli	
	E_Z (GPa)	$E_X = E_Y$ (GPa)	$\nu_{XY} = \nu_{YX}$	$\nu_{ZX} = \nu_{ZY}$	$\nu_{XZ} = \nu_{YZ}$	G_{XY} (GPa)	G_{ZX} (GPa)
Carbon fiber	252	22.30	0.35	0.30	0.027	8.29	22.1
Epoxy	2.03	2.03	0.4	0.4	0.4	0.725	0.725

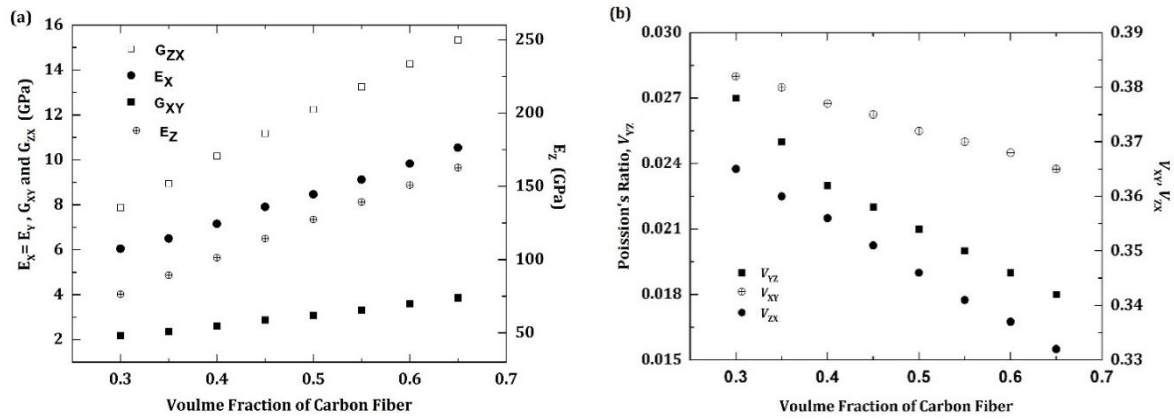


Fig. 6. Materials properties of a single layer of carbon fiber with reinforced polymer matrix composites extracted from modeling: (a) Young moduli, E_x and E_z , and share moduli, G_{xy} , and G_{zx} and (b) Poisson's ratio, ν_{yz} , ν_{xy} , ν_{zx} .

Table 2. Comparison of material properties of Carbon fiber reinforced (carbon fiber of 54.7%) by modeling and experiment

CF 54.7% Vol	Elastic Moduli		Poisson's Ratio			Share Moduli	
	E_Z (GPa)	$E_X = E_Y$ (GPa)	$\nu_{XY} = \nu_{YX}$	$\nu_{ZX} = \nu_{ZY}$	$\nu_{XZ} = \nu_{YZ}$	G_{XY} (GPa)	G_{ZX} (GPa)
Modeling	137.5	8.9	0.372	0.345	0.020	3.56	12.9
Exp	139.42	9.34	0.330	--	--	--	9.29

The uniaxial tensile tests were conducted on 20 layers of the composite of 0.5 mm thickness along x, y and z directions for extracting the mechanical properties i. e. young modulus of E_1 , E_2 , and E_3 and Poisson's ratio of ν_{12} , ν_{21} , ν_{23} , ν_{32} , ν_{31} and ν_{13} . The shear modulus, G_{zx} , of carbon fibers' shear cross-sections is higher than shearing along with carbon fiber longitudinal direction (G_{xy}). However, as carbon fiber volume fraction increases, the Poisson's ratios decrease, which indicates less contraction in the transverse directions under tensile loads. At the fiber-matrix interface with less fiber content, the stress concentration is greater [32]. The variation of fiber concentration is more significant in higher stress regions of the composite layer. In addition, when the fiber concentration is increased, the stress concentration at the fiber decreased and the shear stress at the fiber-matrix interface became more intense. Therefore, the ratio between the matrix and fiber concentration is important, whereas the interfacial stress is

reducing the premature interfacial failure and increases the mechanical properties. The modeling predicted elastic characteristics of the composite are compared with the experimental results [33] and presented in Table 2 which shows a good agreement.

5. Conclusion

In this study, a 20-layer 3D composite with 30-65 vol% carbon fiber was investigated. The modeling results show that Young's modulus in fiber-oriented directions and shear modulus is significantly higher than that of the matrix. The shear modulus of shearing fiber cross-sections is even much higher than the shearing along with fiber longitudinal direction. The carbon fiber volume fraction can enhance structural stability by lowering the composites' Poisson ratios. In this investigation, the modeling results were in good agreement with the experimental data. Several phenomena such as fiber sliding and

fragmentation (which can affect the debonding mechanism) have not been included in the model. Also, time-dependent effects have been neglected for the modeling work. The Mori-Tanaka model is an effective field theory based on Eshelby's elasticity method for inhomogeneity in an infinite medium. The author will consider the two-phase Mori-Tanaka model for predicting the elastic moduli of FRP composites for future work.

Conflict of Interest

The authors declare that there is no conflict of interest regarding the publication of this paper.

Acknowledgments

This computational facility support from the Department of Mechanical and Nuclear Engineering at the University of New Mexico is gratefully acknowledged.

References

- [1] Khalid, M.Y., Rashid, A. Al., Arif, Z.U., Ahmed, W., Arshad, H., Zaidi, A.A., 2021. Natural fiber reinforced composites: Sustainable materials for emerging applications. *Results in Engineering*, 11, pp.100263.
- [2] Khalid, M.Y., Rashid, A. Al., Arif, Z.U., Sheikh, M.F., Arshad, H., Nasir, M.A., 2021. Tensile strength evaluation of glass/jute fibers reinforced composites: An experimental and numerical approach, *Results in Engineering*, 10, pp. 100232.
- [3] Satish, K. G., B. Siddeswarappa, and Kaleemulla, K.M., 2010. Characterization of In-Plane Mechanical Properties of Laminated Hybrid Composites. *Journal of Minerals and Materials Characterization and Engineering*, 09(02), pp.105–14.
- [4] Qatu, M., Abu-Shams, M., Hajianmaleki, M., 2013. Application of laminated composite materials in vehicle design: Theories and analyses of composite beams. *SAE International Journal of Passenger Cars-Mechanical Systems*, 6(2), pp. 1276-1282.
- [5] Sahu, P., Gupta, M., 2017. Sisal (Agave sisalana) fibre and its polymer-based composites: A review on current developments. *Journal of Reinforced Plastics and Composites*, 36(24), pp.1759–80.
- [6] Liew, K. Bin, Goh, C.F., Asghar, S., Syed, H.K., 2021. Overview of Mechanical and Physicochemical Properties of Polymer Matrix Composites. *Encyclopedia of Materials: Composites*: 565–76.
- [7] Khalid, M.Y., Arif, Z.U., Rashid, A. A., Shahid, M.I., Ahmed, W., Tariq, A.F., Abbas, Z., 2021. Interlaminar shear strength (ILSS) characterization of fiber metal laminates (FMLs) manufactured through VARTM process, *Forces in Mechanics*, 4, pp.100038.
- [8] Khalid, M.Y., Rashid, A. A., Sheikh, M.F., 2021. Effect of Anodizing Process on Inter Laminar Shear Strength of GLARE Composite through T-Peel Test: Experimental and Numerical Approach. *Experimental Techniques*, 45, pp.227-235.
- [9] Qayyum, F., Umar, M., Guk, S., Schmidtchen, M., Kawalla, R., Prah, U., 2020. Effect of the 3rd Dimension within the Representative Volume Element (RVE) on Damage Initiation and Propagation during Full-Phase Numerical Simulations of Single and Multi-Phase Steels, *Materials*, 14(1), pp. 42.
- [10] Hassan, M.M., 2016. Effect of Poisson's ratio on material properties characterization by nanoindentation with a cylindrical flat tip indenter (Thesis, South Dakota State University) <https://www.proquest.com/docview/1837117963?accountid=14613>.
- [11] Lomov, S., Perie, G., Ivanov, D., Verpoest, I., Marsal, D., 2011. Modeling three-dimensional fabrics and three-dimensional reinforced composites: challenges and solutions. *Textile Research Journal*, 81(1), pp. 28–41.
- [12] Todoroki, A., Oasada, T., Mizutani, Y., Suzuki, Y., Ueda, M., Matsuzaki, R., Hirano, Y., 2020. Tensile property evaluations of 3D printed continuous carbon fiber reinforced thermoplastic composites. *Advanced Composite Materials*, 29(2), pp.147–62.
- [13] Pan, L., Yapici, U., 2015. A comparative study on mechanical properties of carbon fiber/PEEK composites. *Advanced Composite Materials*, 25(4), pp.359–74.
- [14] Hyer, M.W., 2009. Stress Analysis of Fiber-Reinforced Composite Materials. DEStech Publications, Inc.
- [15] Hu, Z., Hossan, M.R., 2013. Strength evaluation and failure prediction of short carbon fiber reinforced nylon spur gears by finite element modeling. *Applied Composite Materials*, 20(3), pp. 315–30.
- [16] Maligno, A.R., 2008. *Finite element investigations on the microstructure of composite materials* (PhD thesis, University of Nottingham).
- [17] Tham, M.W., Fazita, M.N., Khalil, H., Zuhudi, N.Z., Jaafar, M., Rizal, S., Haafiz, M.M., 2019. Tensile properties prediction of natural fibre composites using rule of mixtures: A review. *Journal of Reinforced Plastics and Composites*, 38(5), pp. 211–48.
- [18] Houshyar, S., Shanks, R.A., Hodzic, A., 2005. The effect of fiber concentration on mechanical and thermal properties of fiber-reinforced polypropylene composites. *Journal of Applied Polymer Science*, 96(6), pp.

- 2260–72.
- [19] Meddad, A., Azaiez, J., Ait-Kadi, A., Nette, R.G., 2002. Micromechanical Modeling of Tensile Behavior of Short Fiber Composites. *Journal of Composite Materials*, 36(04): 423–41.
- [20] Rehan, M.S., Rousseau, J., Gong, X.J., Guillaumat, L., Ali, J.S.M., 2011. Effects of fiber orientation of adjacent plies on the mode I crack propagation in a carbon-epoxy laminates. In *Procedia Engineering*, Elsevier Ltd, pp. 3179–3184.
- [21] Xu, L.R., Hassan, M.M., Anderoglu, O., Zhao, K., Flores, M., 2020. Influence of the stacking sequence on the through-thickness Young's moduli of fibrous composite laminates measured by nanoindentation. *Journal of Composite Materials*, 55(9), pp.1–6.
- [22] Wu, W., Wang, Q., Li, W., 2018. Comparison of tensile and compressive properties of carbon/glass interlayer and intralayer hybrid composites. *Materials*, 11(7).
- [23] Daniel, I.M., 2016. Yield and failure criteria for composite materials under static and dynamic loading. *Progress in Aerospace Sciences*, 81, pp. 18–25.
- [24] Goh, K.L., Aspden, R.M., Mathias, K.J., Hukins, D.W.L., 1999. Effect of fibre shape on the stresses within fibres in fibre-reinforced composite materials. *Proceedings of the Royal Society A: Mathematical, Physical and Engineering Sciences*, 455, pp. 3351–61.
- [25] Deng, X., Hu, J., Wang, W.X., Matsubara, T., 2019. A micromechanical model for the analysis of multidirectional fiber reinforced polymer laminates. *Composite Structures*, 208, pp. 507–16.
- [26] Olivier, P., Cottu, J.P., Ferret, B., 1995. Effects of cure cycle pressure and voids on some mechanical properties of carbon/epoxy laminates. *Composites*, 26(7), pp. 509–15.
- [27] Nirbhay, M., Dixit, A., Misra, R.K., Mali, H.S., 2014. Tensile Test Simulation of CFRP Test Specimen Using Finite Elements. *Procedia Materials Science*, 5, pp.267–73.
- [28] Barbero, E. J., 2008. Finite Element Analysis of Composite Materials USING ANSYS®, Second Edition. CRC Press.
- [29] Vasiliev, V. V., Morozov, E. V., 2018. Advanced mechanics of composite materials and structures. In *Chapter 4-Failure Criteria and Strength of Laminates*, pp.243–94.
- [30] Jawaid, M., Thariq, M., Saba, N., 2018. Failure analysis in biocomposites. *Fibre-Reinforced: Composites and Hybrid Composites*, pp.1-255.
- [31] Daniel, I., Ishai, O., 2006. Engineering mechanics of composite materials. 2nd ed., Oxford University Press.
- [32] Farahikia, M., Macwan, S., Delfanian, F., Hu, Z., 2013. Evaluating the Mechanical Properties of Carbon Fiber Reinforced Polymer Matrix Composite Materials at Room and Elevated Temperatures. *ASME International Mechanical Engineering Congress and Exposition, Proceedings (IMECE)*, pp.1151–58.
- [33] Zubayar, A., 2016. *Mechanical Property Characterization of Polymeric Composites Reinforced by Continuous Microfibers* (MS Thesis, South Dakota State University).